2-8-2005

Two crystal structures of dihydrofolate reductase-thymidylate synthase from Cryptosporidium hominis reveal protein–ligand interactions including a structural basis for observed antifolate resistance

Amy C. Anderson
Dartmouth College

Acta Crystallographica Section F
Structural Biology and Crystallization Communications
ISSN 1744-3091

Two crystal structures of dihydrofolate reductase-thymidylate synthase from *Cryptosporidium hominis* reveal protein–ligand interactions including a structural basis for observed antifolate resistance

Amy C. Anderson

Dartmouth College, Department of Chemistry, Burke Laboratories, Hanover, NH 03755, USA

Correspondence e-mail: aca@dartmouth.edu

Received 18 December 2004
Accepted 21 January 2005
Online 8 February 2005

PDB References: ChDHFR-TS bound to NADPH/DHF/dUMP/CB3717, 1qzf, r1qzfsf; ChDHFR-TS bound to NADPH/1843U89/dUMP, 1sej, r1sejsf.

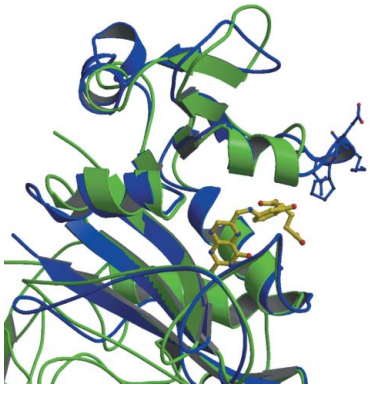

Cryptosporidium hominis is a protozoan parasite that causes acute gastrointestinal illness. There are no effective therapies for cryptosporidiosis, highlighting the need for new drug-lead discovery. An analysis of the protein–ligand interactions in two crystal structures of dihydrofolate reductase-thymidylate synthase (DHFR-TS) from *C. hominis*, determined at 2.8 and 2.87 Å resolution, reveals that the interactions of residues Ile29, Thr58 and Cys113 in the active site of *C. hominis* DHFR provide a possible structural basis for the observed antifolate resistance. A comparison with the structure of human DHFR reveals active-site differences that may be exploited for the design of species-selective inhibitors.

1. Introduction

Cryptosporidium hominis is a water-borne protozoan parasite that infects the intestinal epithelium of many mammals, including humans. This highly infectious agent, recently placed on the Centers for Disease Control list of Class B bioterrorism agents, causes cryptosporidiosis, manifested as self-limiting diarrhea in immune-competent patients and massive chronic diarrhea in immune-deficient patients (Guerrant, 1997; Tzipori, 1998). Despite the threat of cryptosporidiosis infection, to date there are no clinically successful therapies.

Infections from closely related parasitic protozoa such as *Plasmodium falciparum* and *Toxoplasma gondii* have been treated with antifolates, inhibitors of dihydrofolate reductase (DHFR), an essential enzyme in the folate-biosynthetic pathway. DHFR catalyzes the reduction of dihydrofolate using NADPH as a cofactor. In protozoa, a single polypeptide chain codes for both DHFR and thymidylate synthase (TS), forming a bifunctional enzyme. Unfortunately, attempts to treat cryptosporidiosis with antifolates have been unsuccessful. The failure of these drugs has been observed both *in vivo* (Woods *et al.*, 1996) and *in vitro* (Nelson & Rosowsky, 2001). Vasquez *et al.* (1996) found that the sequence of *C. hominis* DHFR (ChDHFR) naturally contains Ile29, Thr58 and Cys113 at the same positions as the antifolate resistance-conferring mutations Ile51, Thr108 and Ile164 in *P. falciparum* DHFR (PfDHFR). The incorporation of these residues in ChDHFR was hypothesized to play an important role in *in vitro* antifolate resistance.

Since the sequence of DHFR has diverged and the sequence of TS has remained largely conserved throughout evolution, it is easier to design parasite-specific DHFR inhibitors instead of TS inhibitors. Therefore, in this work discussion will focus on the ChDHFR domain. In order to design selective and potent ChDHFR inhibitors in future studies, it is necessary to understand ligand binding in ChDHFR including (i) the interactions of the protein with ligands, (ii) the structural effects of the *C. hominis* residues predicted to play a role in antifolate resistance and (iii) ligand-induced conformational changes. Towards that goal, an analysis of two crystal structures of the enzyme DHFR-TS from *C. hominis* is presented. In one structure (structure I), presented in this manuscript, the enzyme is bound to an antifolate inhibitor, 1843U89 (OSI Pharmaceuticals), in the DHFR and TS active sites, as well as NADPH in the DHFR active site and the TS

Table 1
Data and refinement statistics for the structure of ChDHFR-TS/NADPH/1843U89/dUMP.

Values in parentheses are for the highest resolution shell (2.98–2.87 Å).

Space group	*C*2
Unit-cell parameters (Å, °)	a = 214.9, b = 116.3, c = 219.7, β = 95.23
Resolution (Å)	2.87
No. of reflections used	111987
Completeness (%)	90.4 (90)
Redundancy	4.5
$I/\sigma(I)$	8.6 (1.9)
R_{merge}† (%)	10.5 (38.6)
No. of monomers in asymmetric unit	5
Refinement statistics	
R_{cryst}‡ (%)	21.8
R_{free}§ (%)	23.6
Total No. of atoms	21115
No. of water molecules	419
Root-mean-square deviation, bonds (Å)	0.008
Root-mean-square deviation, angles (°)	1.6
Average B factor for non-H atoms (Å^2)	34
Average B factor for water molecules (Å^2)	22
Ramachandran plot statistics	
Residues in most favored regions (%)	84.5
Residues in additional allowed regions (%)	13.8
Residues in generously allowed regions (%)	1.1
Residues in disallowed regions (%)	0.6

† $R_{merge} = \sum |I - \langle I \rangle| / \sum I$. ‡ $R_{factor} = \sum ||F_o| - |F_c|| / \sum |F_o|$. § R_{free} statistics for a test set comprising 10% of the reflections

substrate deoxyuridine monophosphate (dUMP) in the TS active site. In the second structure (structure II), for which details regarding the crystallographic data and refinement have previously been published, the enzyme is bound to the DHFR substrate dihydrofolate (DHF) and the cofactor NADPH in the DHFR active site and dUMP and an antifolate TS inhibitor, CB3717, in the TS active site. This structure formed the basis of previously reported research (O'Neil *et al.*, 2003*a*,*b*) that established that there are two families of DHFR-TS structures from protozoa; analysis of the binding of DHF and NADPH will appear for the first time in this work. A comparison of the structure of ChDHFR-TS with structures of the wild-type and the antifolate-resistant PfDHFR-TS (Yuvaniyama *et al.*, 2003) shows that the ChDHFR residues hypothesized to be important in antifolate resistance have the same effects on the active site as the mutated *P. falciparum* residues known to be important in causing resistance, suggesting equivalent structural effects that decrease the affinity of antifolates. Additionally, a comparison of the two ChDHFR-TS structures reveals no ligand-induced conformational changes in the DHFR active site. A comparison of ChDHFR-TS with human DHFR reveals sites in ChDHFR-TS that may be exploited for the design of parasite-selective inhibitors.

2. Materials and methods

2.1. DHFR activity assays

Enzyme purification has been described previously (O'Neil *et al.*, 2003*a*,*b*). DHFR activity assays were performed using a solution of 50 m*M* TES buffer pH 7.0, 1 m*M* EDTA, 75 µ*M* 2-mercaptoethanol, 1% bovine serum albumin, 1 m*M* dihydrofolate (Eprova) and 100 µ*M* NADPH. Enzyme concentrations were adjusted to give linear initial velocities.

2.2. Crystallization and data collection

Pure enzyme was concentrated to 6.5 mg ml^{-1} and incubated with ligands on ice for 1 h. The final concentrations of the ligands (note that all ligands were dissolved in water with the exception of TMP, which was dissolved in DMSO) were as follows: 1 m*M* TMP and 2 m*M* each of NADPH, dUMP and 1843U89 (OSI Pharmaceuticals). Crystals were grown by hanging-drop vapor diffusion at room temperature and appeared in drops where the reservoir solution contained 100 m*M* Tris pH 8.0, 11% PEG 6K, 50 m*M* ammonium sulfate and 0.2 *M* lithium sulfate. Crystals were transferred to a drop of artificial mother liquor containing 15% ethylene glycol and then transferred to a drop of artificial mother liquor containing 25% ethylene glycol before being frozen in liquid nitrogen.

Diffraction data were collected at 100 K at Stanford Synchrotron Radiation Laboratory beamline 7-1. All data were indexed, integrated and scaled with the *HKL* package (Otwinowski, 1993) and converted to structure factors with *TRUNCATE* (Collaborative Computational Project, Number 4, 1994; see Table 1 for data statistics).

2.3. Structure solution

The structure of ChDHFR-TS bound to 1843U89, NADPH and dUMP was solved by difference Fourier techniques using structure II and refined using *CNS* (Brünger *et al.*, 1998; Table 1). The *R*-factor and R_{free} values, after simulated annealing and manually rebuilding residues surrounding the inhibitors, are 21.8 and 23.6%, respectively. The root-mean-square deviation of bonds is 0.008 Å and the r.m.s.d. for angles is 1.6°.

3. Results and discussion

3.1. Crystallographic structure determination

Structures I and II were solved with diffraction amplitudes extending to 2.87 and 2.8 Å, respectively. The resolution of these structures allows a determination of the proximity of hydrogen-bond donors and acceptors, but detailed measurements of hydrogen bonds will not be included. The determination of structure II has been described previously (O'Neil *et al.*, 2003*a*,*b*; Lilien *et al.*, 2004); structure I was solved using difference Fourier methods and phases from structure II. Electron density for the ligands and residues 3–521

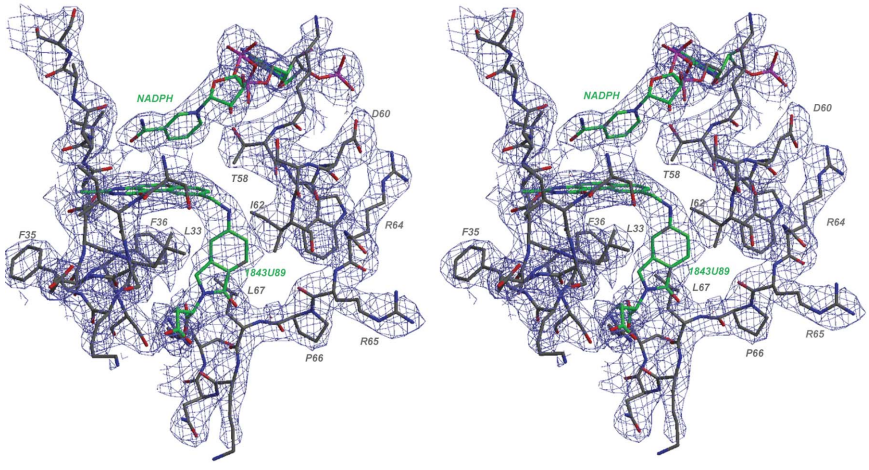

Figure 1
Stereo figure of $2F_o - F_c$ electron density (shown at 2σ contour) for the DHFR active site with the inhibitor 1843U89 and NADPH shown in green.

is well defined (Fig. 1). In the DHFR active site, omit map calculations clearly reveal electron density for 1843U89 in structure I and DHF in structure II, despite the fact that the protein–ligand crystallization mix included the known DHFR inhibitors trimethoprim and methotrexate, respectively. The presence of 1843U89 may be explained by results from a ChDHFR assay showing that 1843U89 exhibits a 50% inhibition (IC_{50}) value of 5 μM, threefold tighter binding than trimethoprim (IC_{50} = 14 μM). The presence of DHF may be explained by the fact that the protein was immediately crystallized after 2 mM DHF elution from the methotrexate agarose column.

ChDHFR-TS assembles as a dimer. In the asymmetric unit, one dimer is coincident with the crystallographic twofold axis and two dimers are located away from the axis, yielding five monomers per asymmetric unit. The quality of the electron density in all five monomers is essentially identical. The protein monomers were refined using non-crystallographic symmetry restraints.

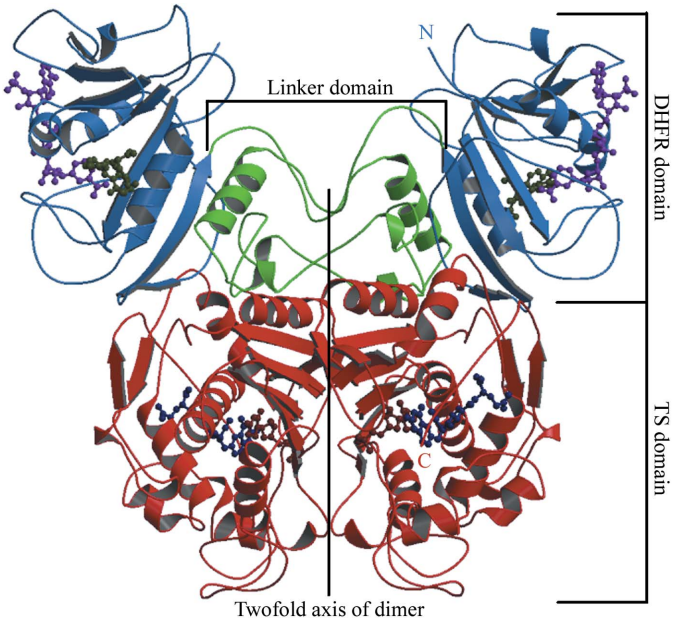

Figure 2
An overview of the structure of ChDHFR-TS. The DHFR domains are shown in blue, the linker domains are shown in green and the TS domains are shown in red. The ligands are shown in ball-and-stick representation.

3.2. Overall description of the DHFR-TS structure

ChDHFR-TS is a bifunctional protein organized with the N-terminal DHFR domain separated from the C-terminal TS domain by a 59-residue linker domain (Fig. 2). After folding the DHFR domain (1–175), residues from the linker domain (176–206) cross from one monomer of the dimer to the other and form a helix, called the donated helix, which packs against the opposite DHFR active site. The interactions of the donated helix with the opposite monomer have been described in detail in a previous publication (O'Neil *et al.*, 2003*a*,*b*). The linker then crosses back to the originating monomer, forming a ninth strand in the β-sheet of DHFR, and then forms the TS domain (residues 207–521; O'Neil *et al.*, 2003*a*,*b*). In the crystal structures described here, ChDHFR has features that define the closed conformation of *P. carinii* DHFR (PcDHFR; Cody *et al.*, 1999), suggesting that ChDHFR is in the closed conformation.

3.3. Ligand binding in ChDHFR-TS

NADPH is bound to ChDHFR in an extended conformation (Figs. 3*a* and 3*b*). There are several hydrophobic interactions between NADPH and ChDHFR, including Ile75 and Ile118 with the adenosine, and Leu25, Ile19, Thr58, Tyr119, Gly115 and the pteridine ring of dihydrofolate or the benzoquinazoline ring of 1843U89 with the nicotinamide ring. Several potential hydrogen bonds are also apparent: Ser76, Ser77 and Arg56 with the O atoms of the adenosyl phosphate, Thr58 and Ser117 with the O atoms of the bridge phosphate and the backbone of Ala11 with the amino and keto oxygen groups of the nicotinamide ring.

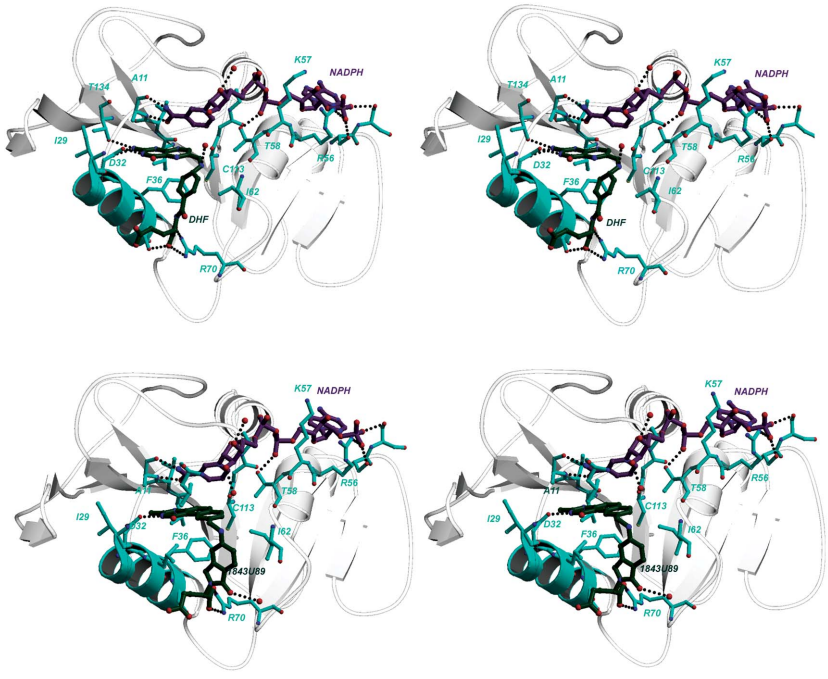

Figure 3
Stereoviews of the active sites bound to ligands. (*a*) ChDHFR bound to NADPH and 1843U89, (*b*) ChDHFR bound to NADPH and DHF. Potential hydrogen bonds are shown with dashed lines and ordered solvent molecules are shown as red spheres. The DHFR helix containing Ile29 and Asn32 is shown in cyan.

The antifolate 1843U89 (OSI Pharmaceuticals), originally developed as an anticancer TS inhibitor, is bound in the DHFR active site of structure I (Fig. 3*a*). One hydrogen bond is formed from the benzoquinazoline ring to Asp32 and the methyl group on that ring is buried in a small hydrophobic pocket comprised of Thr134, Ala11 and Val9. Phe36, Leu25 and Ile62 form other hydrophobic contacts with the benzoquinazoline ring. The isoindolinone moiety is bound in a highly hydrophobic pocket comprised of Leu67, Ile62, Met54, Leu33, Phe36 and Leu25. The folate tail makes two potential hydrogen bonds with Arg70 and one with an ordered water molecule.

Interestingly, 1843U89 is bound in both the DHFR and TS active sites of structure I. It is noteworthy that both sites include a predominance of hydrophobic interactions. In fact, there

are no potential hydrogen bonds between 1843U89 and *C. hominis* TS and only four in ChDHFR, despite the number of hydrogen-bond donors and acceptors in 1843U89.

Dihydrofolate is bound to ChDHFR in the same conformation as in the human enzyme (PDB code 1drf; Oefner *et al.*, 1988; Fig. 3*b*). The pteridine ring forms three hydrogen bonds with the protein: one from the amino group to Thr134, another from the ring NH to the carboxylate of Asp32 and a third from the amino group to Asp32. The pteridine ring also has extensive van der Waals contacts with Phe36, Val9 and the nicotinamide ring. The *para*-aminobenzoic acid (*p*ABA) binds in the same location as the isoindolinone ring of 1843U89 and makes many of the same hydrophobic interactions with the protein. There are three potential hydrogen bonds formed between the glutamate tail of dihydrofolate and the protein: two bonds with Arg70 and a unique hydrogen bond relative to other species with the side chain of Ser37.

3.4. Structural effects of residues predicted to be important in antifolate resistance

Using a comparison of the structures of wild-type and resistant PfDHFR-TS, Yuvaniyama and coworkers determined many of the structural effects of the PfDHFR mutations known to cause antifolate resistance (Yuvaniyama *et al.*, 2003). Vasquez *et al.* (1996) used a sequence alignment (Fig. 4) to show that residues Ile29, Thr58 and Cys113 are at the same positions as the mutations Ile51, Asn108 and Leu164 in resistant PfDHFR. A comparison of ChDHFR with the structures of wild-type PfDHFR and the quadruple mutant (Asn51Ile, Cys59Arg, Ser108Asn, Ile164Leu) PfDHFR (Yuvaniyama *et al.*, 2003) (Fig. 5) reveals that ChDHFR residues Ile29, Thr58 and Cys113 have equivalent structural perturbations on the active site.

```
Ch      MSEKNVSIVV AASVLS---- ---------- --SGIGINGQ LPWS-ISEDL KFFSKITNNK 43
Hu        VGSLNCIV AVSQN----- ---------- --MGIGKNGD LPWPPLRNEF RYFQRMTTTS 41
Pf MMEQVCDVFDIYAIC ACCKVESKNE GKKNEVFNNY TFRGLGNKGV LPWKCNSLDM KYFCAVTTYV 65

Ch CDSN------ ---------- ---------- --KKNALIMG RKTWDSIGRR --PLKNRIIV  73
Hu SVEG------ ---------- ---------- --KQNLVIMG KKTWFSIPEK NRPLKGRINL  73
Pf NESKYEKLKY KRCKYLNKET VDNVNDMPNS KKLQNVVVMG RTSWESIPKK FKPLSNRINV 125

Ch VISSSLPQDE ADPNVVVFRN LEDSIENLMN DDSIEN---I FVCGGESIYR DALKDNFVDR 130
Hu VLSRELKEPP QGAH-FLSRS LDDALKLTEQ PELANKVDMV WIVGGSSVYK EAMNHPGHLK 132
Pf ILSRTLKKED FDEDVYIINK VEDLIVLLGK LNYYK----C FIIGGSVVYQ EFLEKKLIKK 181

Ch IYLTRVALED IEFDTYFPEI PET-FLPVYM S-----QTFC TKNISYDFMI FEKQEKKTLQ 184
Hu LFVTRIMQDF ESD-TFFPEI DLEKYKLLPE YPGVLSDVQE EKGIKYKFEV YEKND      186
Pf IYFTRINSTY EC-DVFFPEI NENEYQIISV S-----DVYT SDDTTLDFII YKKTN      230
```

Figure 4
Sequence alignment of the DHFR domains from *C. hominis* (Ch), human (Hu) and *P. falciparum* (Pf; wild type). The PEKN region is shown in a green box; the residues involved in antifolate resistance in *P. falciparum* and *C. hominis* are shown in red.

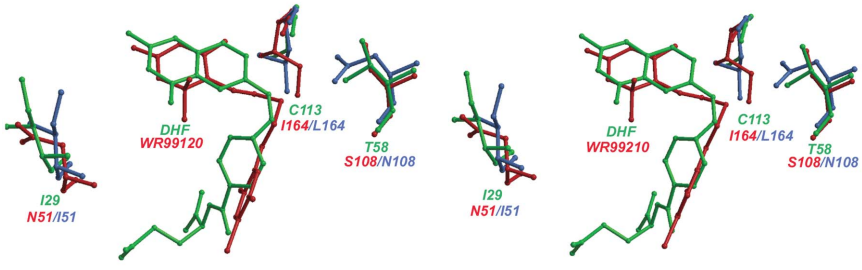

Figure 5
Stereoview of a superposition of DHF from structure II of ChDHFR (green) and three residues from ChDHFR predicted to be important in causing antifolate resistance (Ile29, Thr58 and Cys113 in green) with residues from wild-type PfDHFR (red), the inhibitor WR99210 (red) and resistant PfDHFR (blue).

Wild-type PfDHFR contains Asn51, which forms a hydrogen bond with the backbone amide of the active-site Asn, which in turn forms hydrogen bonds with the diaminopyrimidine of most antifolate inhibitors. Ile29 (ChDHFR) and the resistance mutation Ile51 (PfDHFR) superimpose; both lose the hydrogen bond with the active-site Asn, creating a backbone shift at the active site. Thr58 in ChDHFR superimposes with the PfDHFR mutation Asn108. Asn108 creates steric interactions with the nicotinamide ring of NADPH and the *para*-chlorophenyl group of pyrimethamine (Yuvaniyama *et al.*, 2003). The same interactions are apparent for Thr58 in ChDHFR. Finally, in PfDHFR the Ile164Leu mutation causes an additional sevenfold reduction in binding to pyrimethamine (Sirawaraporn *et al.*, 1997), presumably owing to reduced van der Waals contacts. In ChDHFR, Cys113 exhibits an even greater reduction in van der Waals contacts (Fig. 5), possibly severely decreasing antifolate affinity.

Evidence from field isolates (Basco *et al.*, 1996) and *in vitro* experiments (Sirawaraporn *et al.*, 1997) shows that the appearance of multiple mutations in resistant strains of *Plasmodium* has a synergistic effect in decreasing the affinity of antifolate inhibitors. For example, the Ser108Thr mutation by itself does not lead to a high degree of resistance, but this mutation in combination with Ala16Thr leads to high levels of cycloguanil resistance (Foote *et al.*, 1990; Peterson *et al.*, 1990). The same argument may apply to *C. hominis*: a single residue may not contribute more than a slight increase in the binding constant of an inhibitor, but the accumulation of multiple residues may cause a significant loss of affinity. In ChDHFR, the decreased van der Waals surface of Cys113, the steric interactions of Thr58 and the loss of a key hydrogen bond from Ile29 may together lead to a pronounced decrease in antifolate binding.

3.5. Ligand-induced conformational changes

A comparison of ChDHFR bound to DHF and 1843U89 surprisingly reveals that there are few conformational changes in the protein induced by the differences between DHF and 1843U89. The benzoquinazoline ring of 1843U89 fits into the same space as the CH_2N bridge of DHF. The isoindolinone appears to be accommodated in a greater volume of the hydrophobic pocket and forms contacts with Ile62, Leu67, Leu33 and Phe36. In comparison, the *p*ABA ring of DHF contacts the same residues, with the exception of Leu67.

3.6. Selectivity: comparison with human DHFR

A superposition of the structures of ChDHFR with DHFR from human (PDB code 1drf; Oefner *et al.*, 1988), *P. carinii* (PDB code 2cd2; Cody *et al.*, 1999) and *Escherichia coli* (PDB code 1rb3; Sawaya & Kraut, 1997) shows strong conservation of the overall conformation of DHFR, but also reveals a significant difference between ChDHFR, PcDHFR and human DHFR. Human DHFR has a loop (residues 63–65 and sequence Pro-Glu-Lys-Asn, PEKN) near the exit to the active site; this loop is deleted in ChDHFR (Figs. 4 and 6). The conformation of the PEKN loop and the initial proline residue is conserved in most other eukaryotic DHFR species. The proline in the human DHFR structure (Oefner *et al.*, 1988) is only 4 Å from the *p*ABA ring of dihydrofolate and forms van der Waals contacts with the ring.

Two other active-site residues differ between ChDHFR and human DHFR: Val9 and Leu33 in ChDHFR are Ile7 and Phe31, respectively, in

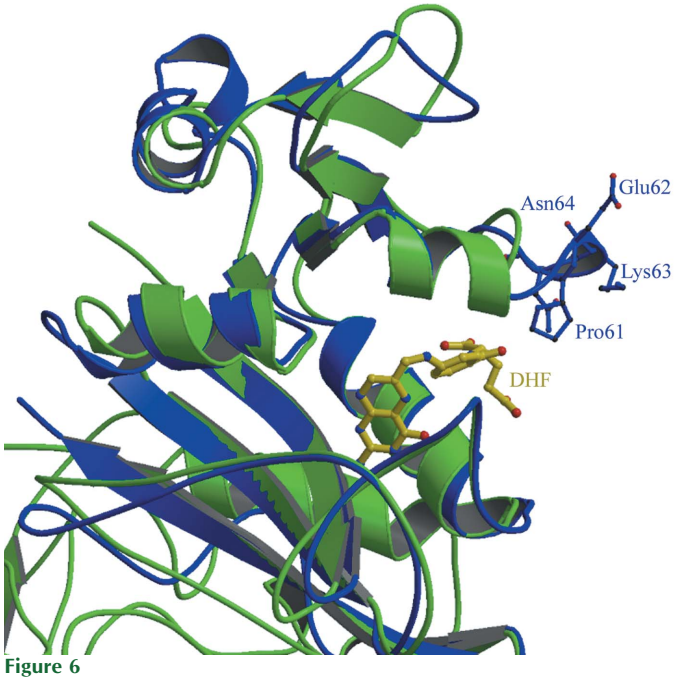

Figure 6
The structure of the PEKN loop in human DHFR. The structure of human DHFR is shown in blue; the structure of ChDHFR is shown in green. Dihydrofolate (DHF) is shown in yellow as a reference to the location of the active site.

human DHFR. The valine substitution has reduced van der Waals contact with the pteridine ring in structure II. The substitution of Leu33 relative to Phe31 in the human enzyme has been implicated in the selectivity of trimethoprim for parasitic and bacterial species over human (Kuyper *et al.*, 1985; Roth *et al.*, 1987).

In summary, the two structures of ChDHFR-TS reveal the interactions of residues in the DHFR domain with different ligands, show that the structural effects of the residues implicated in antifolate resistance are similar to the structural effects of the mutations found in resistant strains of *P. falciparum* and also reveal key structural differences with human DHFR. The information discovered here will be valuable in the design of potent and selective ChDHFR inhibitors.

This work is supported by a grant to ACA from the National Institutes of Health (GM-067542). The author acknowledges Robert O'Neil for his contributions to data collection and structure determination and Dr Rick Nelson (San Francisco General Hospital) for providing the expression plasmid containing the *C. hominis* DHFR-TS gene.

References

Basco, L., Pecoulas, P., LeBras, J. & Wilson, C. (1996). *Exp. Parasitol.* **82**, 97–103.
Brünger, A. T., Adams, P. D., Clore, G. M., DeLano, W. L., Gros, P., Grosse-Kunstleve, R. W., Jiang, J.-S., Kuszewski, J., Nilges, M., Pannu, N. S., Read, R. J., Rice, L. M., Simonson, T. & Warren, G. L. (1998). *Acta Cryst.* D**54**, 905–921.
Cody, V., Galitsky, N., Rak, D., Luft, J., Pangborn, W. & Queener, S. (1999). *Biochemistry*, **38**, 4303–4312.
Collaborative Computational Project, Number 4 (1994). *Acta Cryst.* D**50**, 760–763.
Foote, S., Galatis, D. & Cowman, A. (1990). *Proc. Natl Acad. Sci.* **87**, 3014–3017.
Guerrant, R. (1997). *Emerg. Infect. Dis.* **3**, 51–57.
Kuyper, L., Roth, B., Baccanari, D., Ferone, R., Beddell, C., Champness, J., Stammers, D., Dann, J., Norrington, F., Baker, D. & Goodford, P. (1985). *J. Med. Chem.* **28**, 303–311.
Lilien, R., Bailey-Kellogg, C., Anderson, A. & Donald, B. (2004). *Acta Cryst.* D**60**, 1057–1067.
Nelson, R. & Rosowsky, A. (2001). *Antimicrob. Agents Chemother.* **45**, 3293–3303.
Oefner, C., D'Arcy, A. & Winkler, F. (1988) *Eur. J. Biochem.* **174**, 377–385.
O'Neil, R., Lilien, R., Donald, B., Stroud, R. & Anderson, A. (2003*a*). *J. Biol. Chem.* **278**, 52980–52987.
O'Neil, R., Lilien, R., Donald, B., Stroud, R. & Anderson, A. (2003*b*). *J. Eukaryot. Microbiol.* **50**, 555S–556S.
Otwinowski, Z. (1993). *Proceedings of the CCP4 Study Weekend. Data Collection and Processing*, edited by L. Sawyer, N. Isaacs & S. Bailey, pp. 56–62. Warrington: Daresbury Laboratory.
Peterson, D., Milhous, W. & Wellems, T. (1990). *Proc. Natl Acad. Sci. USA*, **87**, 3018–3022.
Roth, B., Rauckman, B., Ferone, R., Baccanari, D., Champness, J. & Hyde, R. (1987). *J. Med. Chem.* **30**, 348–356.
Sawaya, M. R. & Kraut, J. (1997). *Biochemistry*, **36**, 586–603.
Sirawaraporn, W., Sathitkul, T., Sirawaraporn, R., Yuthavong, Y. & Santi, D. (1997). *Proc. Natl Acad. Sci. USA*, **94**, 1124–1129.
Tzipori, S. (1998). *Adv. Parasitol.* **40**, 187–221.
Vasquez, J., Gooze, L., Kim, K., Gut, J., Petersen, C. & Nelson, R. (1996). *Mol. Biochem. Parasitol.* **79**, 153–165.
Woods, K., Nesterenko, M. & Upton, S. (1996). *Ann. Trop. Med. Parasitol.* **90**, 603–615.
Yuvaniyama, J., Chitnumsub, P., Kamchonwongpaisan, S., Vanichtanankul, J., Sirawaraporn, W., Taylor, P., Walkinshaw, M. & Yuthavong, Y. (2003). *Nature Struct. Biol.* **10**, 357–365.